ISSN 0036-0236, Russian Journal of Inorganic Chemistry, 2016, Vol. 61, No. 1, pp. 11–17. © Pleiades Publishing, Ltd., 2016.
Original Russian Text © D.B. Chugunov, L.L. Meshkov, K.B. Kalmykov, A.K. Osipov, 2016, published in Zhurnal Neorganicheskoi Khimii, 2016, Vol. 61, No. 1, pp. 13–19.

SYNTHESIS AND PROPERTIES OF INORGANIC COMPOUNDS

Synthesis of Quasi-Crystalline Phases in the Al–Cu–Fe–Cr System

D. B. Chugunov[a], L. L. Meshkov[b], K. B. Kalmykov[b], and A. K. Osipov[a]

[a]*Ogarev Mordovia State National Research University, ul. Bol'shevistskaya 68, Saransk, Mordovia, 430005 Russia*
[b]*Chair of General Chemistry, Chemical Faculty, Lomonosov Moscow State University, Vorob'evy gory, Moscow, 119992 Russia*
e-mail: iman081@gmail.com

Received June 5, 2015

Abstract—Phase equilibria in the Al–Cu–Fe system alloyed with 5% Cr were studied. Based on the data of X-ray powder diffraction analysis, electron microscopy, and differential thermal analysis, the effect of temperature on $i \Leftrightarrow d$ phase transitions in alloys $Al_{65}Cu_{25}Fe_5Cr_5$ and $Al_{70}Cu_{20}Fe_5Cr_5$. In the Al–Cu–Fe–Cr system, multiphase structures were detected; these structures are mixtures of quasi-crystalline and approximant phases, the contents and morphologies of which depend on the composition of the initial mixture and the crystallization rate.

DOI: 10.1134/S003602361601006X

Quasi-crystalline (QC) compounds attract the attention of researchers because their properties are of technological interest [1]. Among such compounds, there are a number of aluminum alloys, which have found practical use [2]. High brittleness and low plasticity are the main disadvantages of using QC compounds as structural materials. However, it is due to their brittleness that they can readily be mechanically powdered and used as fillers in composite materials, and also as corrosion-resistant and antifriction coatings [3, 4]. Among crystalline phases experiencing mutual transformations with QC phases, there is a group of phases the atomic structure of which is close to the local atomic structure of QC phases. This group contains rational and structural approximant crystalline (AC) phases [5, 6].

One issue still being debated is the sequence of the formation of phases in ordinary crystallization of melts the compositions of which are similar to the region of the existence of QC phases. For example, in the Al–Cu–Fe system [7], in which the *i*-phase (ico-phase) is stable [8–10], the diffusion transformation $(\lambda + \beta) + L \Leftrightarrow i$ occurs only in subsequent annealings of multiphase $(\lambda + \beta + i + \theta)$ cast alloys. In some cases, quasi-crystals reversibly change to binary AC phases, which produce electron diffraction patterns resembling those of QC phases. Specifically, the transformation of the *i*-phase $Al_{62}Cu_{25.5}Fe_{12.5}$ into the crystalline bcc phase β-Al(CuFe) with the unit cell parameter $a = 0.2911$ nm was detected [6, 7]. This group of structures contains the following binary phases: the monoclinic λ-$Al_{13}Fe_4$ ($a = 1.5492$ nm, $b = 0.8078$ nm, $c = 1.2471$ nm, $\beta = 107.69°$) [7], the tetragonal θ-phase (Al_2Cu) with the unit cell parameters $a = 0.6066$ nm and $c = 0.4874$ nm [7], and the orthorhombic ζ-phase (Al_3Cu_4) ($a = 0.8127$ nm, $b = 1.4199$ nm, $c = 0.9993$ nm) [5] in the aluminum–copper system; the group also includes the ternary ψ-phase ($Al_{10}Cu_{10}Fe$). A multiphase structure containing several related phases can be thermally rearranged into a single-phase QC state [10, 11]. Therefore, the technology for producing a QC phase in the Al–Cu–Fe system often includes a stage of crystallization from melt [12].

In the Al–Cu–Cr ternary system, quasi-crystals also form [12, 13]. The formation of quasi-crystals of two types was established: *i*-phase was found in a rapidly annealed alloy of the composition $Al_{65}Cu_{20}Cr_{15}$, but was not produced after ordinary solidification of the alloy of this composition [14, 15]. The formation of QC phases of the *d*-type (*deca*-phase) of various compositions was described before [16].

There are relatively few published studies of the effect of alloying on the stability of the ternary *i*-phase Al_6Cu_2Fe [17–19] with the unit cell parameters $a = 1.4868$ nm, $b = 1.6849$ nm, $c = 1.6024$ nm [20]. There is next to no data on phase equilibria in quaternary state diagrams describing QC compounds.

Investigation of transformations in cast alloys in the Al–Cu–Fe–Cr system is necessary for determining the relationship between the detected microstructure of QC materials and their physicochemical properties [21]. The purpose of this work was to determine the sequence of the formation of QC phases in alloys of the composition $Al_{65}Cu_{25}Fe_{10}$, alloyed with chromium, using a set of physicochemical methods. The development of modes of reproducible synthesis of QC phases in multicomponent alloys based on aluminum is a topical challenge.

EXPERIMENTAL

The samples were prepared from metal powders: 99.9% pure Al, electrolytic copper, carbonyl iron, and electrolytic refined chromium. The alloy was obtained by triple melting of a weighed (2 g) sample of metal powders in an electric-arc furnace in an argon atmosphere, with each of the three meltings lasting 15 s.

The microstructural analysis and the determination of the elemental composition of the samples were performed with a LEO EVO-50 XVP scanning electron microscope (Karl Zeiss) with an INCA Energy 450 energy dispersive analysis system (EDX) (Oxford Instruments) at an accelerating voltage of 15 kV.

The X-ray powder diffraction analysis was made with an Empyrean X-ray diffractometer (PANalytical) within the angle range $20° \leqslant 2\theta \leqslant 95°$ at a step size of 0.01° using CuK_α radiation with a 16-mm automatic slit. The results were reduced to a constant slit width of 1°; the X-ray powder diffraction patterns were processed using the HighScorePlus software. Quantitative X-ray powder diffraction analysis was carried out by the Rietveld method using the PHAN% program [24].

The calorimetric (DSC) curves of the samples were recorded with a Netzsch STA 449 F1 Jupiter simultaneous thermal analyzer within the temperature range 25–920°C at a heating rate of 20 K/min. The samples were annealed in a calorimeter until a given temperature was reached, after which the heating was terminated and the samples were cooled at a rate of 50 K/min.

RESULTS AND DISCUSSION

In most of the ternary aluminum systems, the crystallization of alloys in the concentration region of the existence of QC phases occurs by a peritectic reaction. It was found [8] that the metal melts from which phases crystallize are chemically inhomogeneous. In these melts, atomic combinations of various chemical compositions form; and in the melt in which during solidification *i*-phase forms, there are clusters with forbidden symmetry [22]. As is known [9], in the Al–Cu–Fe system early in the crystallization, there is primary crystallization of solid crystalline phases λ-$Al_{13}Fe_4$ and β-Al(CuFe) from liquid. For an invariant peritectic reaction, there should be interdiffusion of elements from solid phases into the melt, from which new phases are further separated. An insignificant change in the melt composition leads to a significant change in the resultant microstructure (Fig. 1).

According to the data of this work, after the electric-arc melting in ternary alloys in the Al–Cu–Fe system, a typical dendritic morphology forms, which is constituted by λ-particles of irregular shape, surrounded by a gray QC phase. Between them is the β-phase Al(CuFe). Table 1 presents the qualitative and quantitative compositions. It was previously noted that multiphase structures are mixtures of QC and AC phases, the contents and morphologies of which depend on the crystallization mode. A mixture completely transforms into a quasi-crystalline *i*-phase as a result of short-term isothermal annealings at 800°C of mechanically ground alloy $Al_{64}Cu_{24}Fe_{12}$ under optimal conditions of heat treatment [11].

Alloying of the ternary alloy with 5 at % chromium dramatically changes the course of the alloy crystallization. In the sample, the λ-$Al_{13}Fe_4$ phase was not found; instead of it, the binary θ-phases (2%) of the compositions Al_2Cu and β-Al(CuFe) form at a content of 11%. The distribution of QC phases is characterized by certain morphological features. For example, the abundantly forming dark-gray *d*-phase (74.4%) is surrounded by a layer of the gray *i*-phase (13.1%) (Fig. 2a). This can probably be explained by

Table 1. Results of energy-dispersive X-ray spectroscopy and the unit cell parameters of the studied alloys

Composition of sample	Phase	wt %	*a*	*b*	*c*	Concentration, at %			
			Å			Al	Cu	Fe	Cr
$Al_{70}Cu_{20}Fe_5Cr_5$	Al(CuFe)	3.1				53.4	43.9	1.9	0.8
	Al_2Cu	14.4	6.04		4.86	64.3	34.6	0.8	0.3
	d	82.5	23.67	12.29	32.47	71.4	11.2	6.8	10.6
$Al_{65}Cu_{25}Fe_5Cr_5$	Al(CuFe)	10.7	2.91			50.1	46.4	2.7	0.8
	Al_2Cu	1.8	6.08		4.89	64.3	35.1	0.3	0.3
	i	13.1	14.86	16.83	16.02	65.0	22.5	6.6	5.9
	d	74.4	23.71	12.91	32.53	67.1	16.4	8.4	8.1
$Al_{65}Cu_{25}Fe_{10}$	β	26.4	2.91			54.5	41.4	4.1	
	i	49.8	14.85	16.82	16.03	60.8	24.5	14.7	
	λ	23.8	15.36	8.12	12.54	66.5	4.6	28.9	

local isomorphism of these QC structures, which manifests itself in the coherence of the surfaces of their grains, and by nonequilibrium crystallization [15].

Figure 2b presents the microstructure of a cast sample of the composition $Al_{70}Cu_{20}Fe_5Cr_5$ with higher aluminum content. Importantly, no *i*-phase was found in the cast sample. The sample, as well as $Al_{65}Cu_{25}Fe_5Cr_5$, has multiphase structure. According to the X-ray powder diffraction analysis (Fig. 3), after crystallization, the structure contains much (82.5%) *d*-phase. Much more Al_2Cu forms (14.4%). Because the Al(CuFe) content is low, the intensity of the reflections of this phase in the X-ray powder diffraction pattern is insignificant. The totality of the data of scanning electron microscopy and X-ray powder diffraction analysis showed that the *d*-phase can form directly in melt crystallization. Note also that the microstructural analysis data agree well with the X-ray powder diffraction analysis data and the published data [11].

To determine the effect of temperature on the structure stability, the thermal analysis of the alloys was made within the range 20–920°C at a heating rate of 20 deg/min.

The calorimetric curve of $Al_{65}Cu_{25}Fe_{10}$ exhibits several endothermic events related to the decomposition of intermetallic phases forming in ingot crystallization. The first endothermic peak with a magnitude of 3.4 J/g within the temperature range 590–600°C is likely to be related to the decomposition of intermetallic compounds Al_2Cu and Cu_xAl_y [23]. The second, higher and narrower, peak characterized by a high

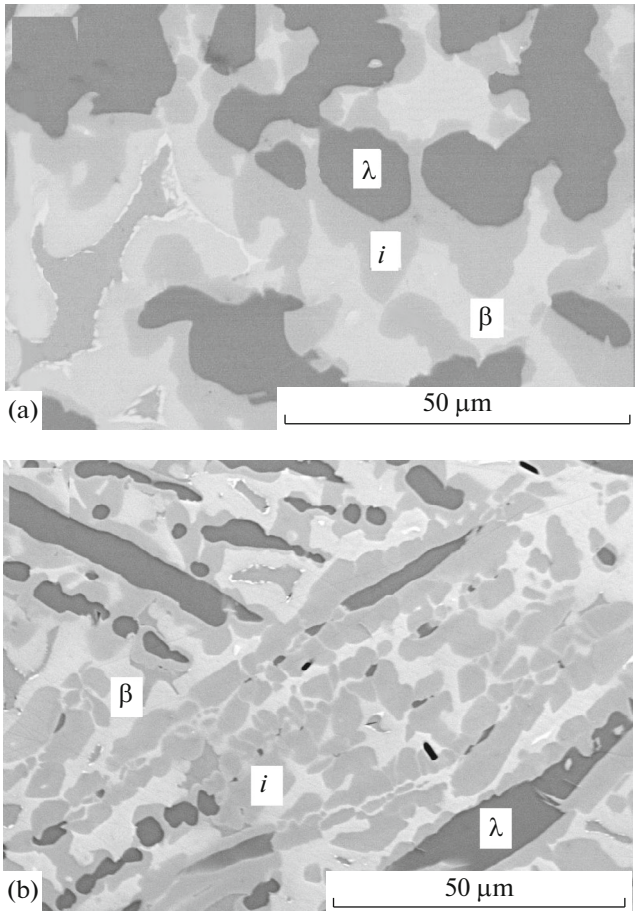

Fig. 1. Micrographs of cast samples of the compositions (a) $Al_{64}Cu_{24}Fe_{12}$ and (b) $Al_{65}Cu_{25}Fe_{10}$.

Table 2. Compositions and contents of phases in samples of the compositions $Al_{70}Cu_{20}Fe_5Cr_5$, $Al_{65}Cu_{25}Fe_5Cr_5$, and $Al_{65}Cu_{25}Fe_{10}$ after heat treatment (HT)

Composition	Phase	HT temperature, °C					
		without HT	580	650	740	920	
		Percentage content (±0.7%)					
$Al_{70}Cu_{20}Fe_5Cr_5$	Al_2Cu	14.4	9.9	5.6	5.1	8.1	
	β	3.1	–	5.6	7.3	8	
	d	82.5	90.1	88.8	82.8	73.7	
	i	–	–	–	4.8	10.2	
$Al_{65}Cu_{25}Fe_5Cr_5$		HT temperature, °C					
		without HT	580	600	690	820	920
	Al_2Cu	1.8	–	–	–	–	–
	β	10.7	5.8	5.7	4.6	5.2	6.9
	d	74.4	82.0	82.2	95.4	94.8	93.1
	i	13.1	12.2	12.1	–	–	–
$Al_{65}Cu_{25}Fe_{10}$		HT temperature, °C					
		without HT	675	710	920		
	β	26.4	23.6	14.2	9.9		
	i	49.8	56.5	72.2	90.1		
	λ	23.8	19.9	13.6	–		

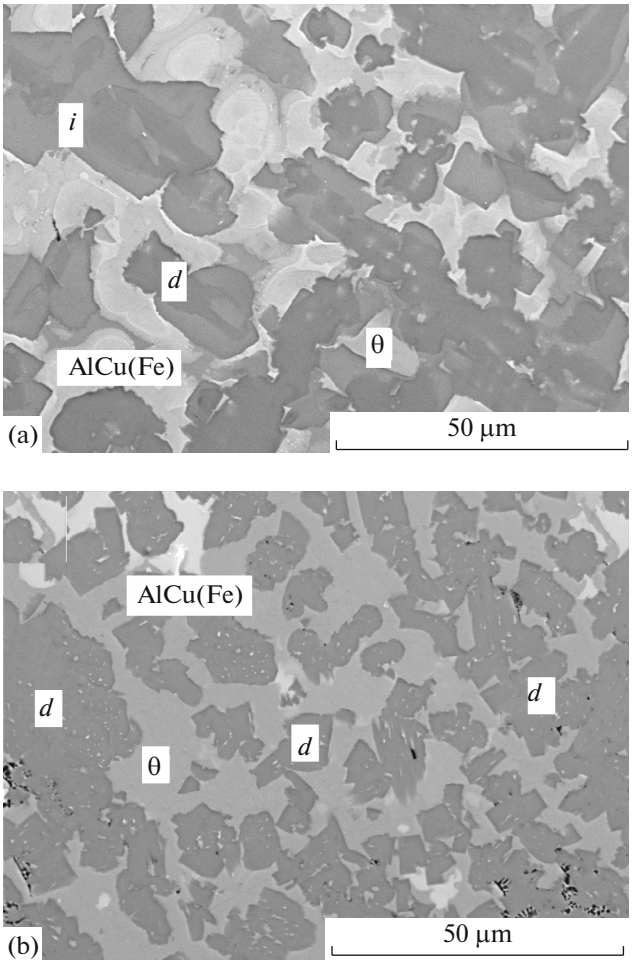

Fig. 2. Micrographs of cast samples of the compositions (a) $Al_{65}Cu_{25}Fe_5Cr_5$ and (b) $Al_{70}Cu_{20}Fe_5Cr_5$.

(18.3 J/g) heat absorption at ~700°C indicates the beginning of the peritectoid transformation (λ + β) + L ⇔ *i*. The third, weak, peak at 875°C corresponds to the decomposition of the QC *i*-phase.

Figure 4 presents the differential scanning calorimetry of the studied samples in the Al–Cu–Fe–Cr system containing 5 at % Cr. The heat release curve of the sample of the composition $Al_{65}Cu_{25}Fe_5Cr_5$ to exhibit an insignificant endothermic peak at 600°C. Two other exothermic peaks are shifted toward higher temperatures 600–800°C. The heat release decreases from 13.4 to 8.9 J/g with increasing temperature. The presence of two successive peaks suggests that the mixture while heating undergoes two similar phase transformations. The heat release is generally related to the number *i* ⇔ *d* of metastable intermediate phases forming within this temperature range. This conclusion is confirmed by the data of X-ray powder diffraction analysis (Fig. 5; Table 2).

Alloy $Al_{70}Cu_{20}Fe_5Cr_5$ within the temperature range 587–639°C is characterized by the double endothermic peak with a heat absorption of 85.7 J/g, which is likely to correspond to the melting of the β-phase. This is indicated by the X-ray powder diffraction analysis data (Fig. 6) demonstrating a noticeable change in the intensities of the reflections of the phases Al_2Cu and Al(CuFe). As is seen, while heating the quaternary alloy, the signs of the heat changes in the sequence of phase transitions remain unchanged. In the calorimetric curve of this alloy, there is a diffuse exothermic peak at 720°C, coinciding with the beginning of the formation of the *i*-phase, which agrees with the published data [12].

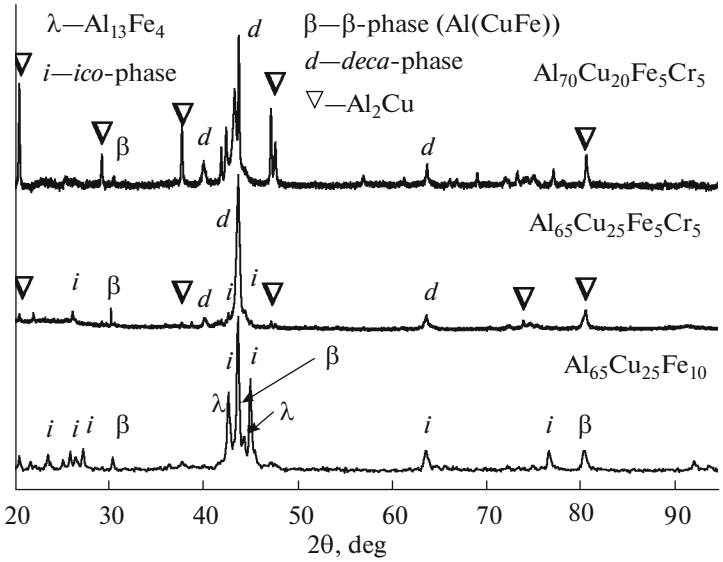

Fig. 3. X-ray powder diffraction patterns of cast samples of the compositions $Al_{65}Cu_{25}Fe_{10}$, $Al_{65}Cu_{25}Fe_5Cr_5$, and $Al_{70}Cu_{20}Fe_5Cr_5$.

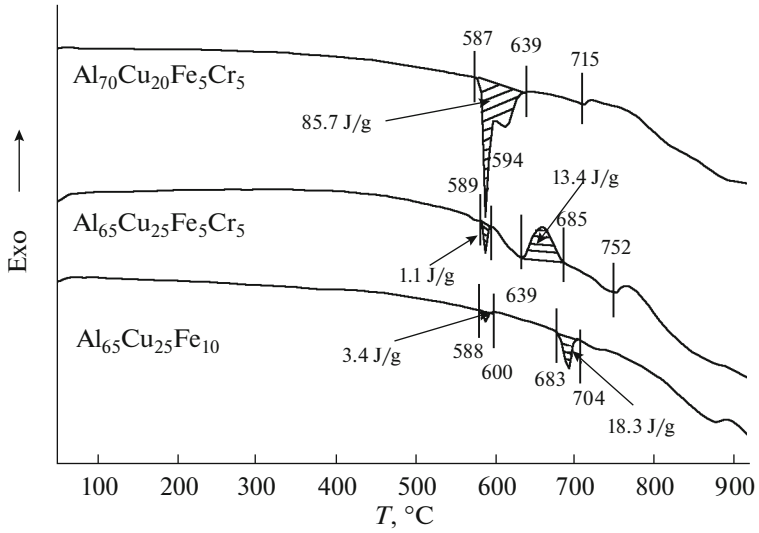

Fig. 4. Calorimetric curves of heat release in alloys of the compositions $Al_{65}Cu_{25}Fe_{10}$, $Al_{65}Cu_{25}Fe_5Cr_5$, and $Al_{70}Cu_{20}Fe_5Cr_5$.

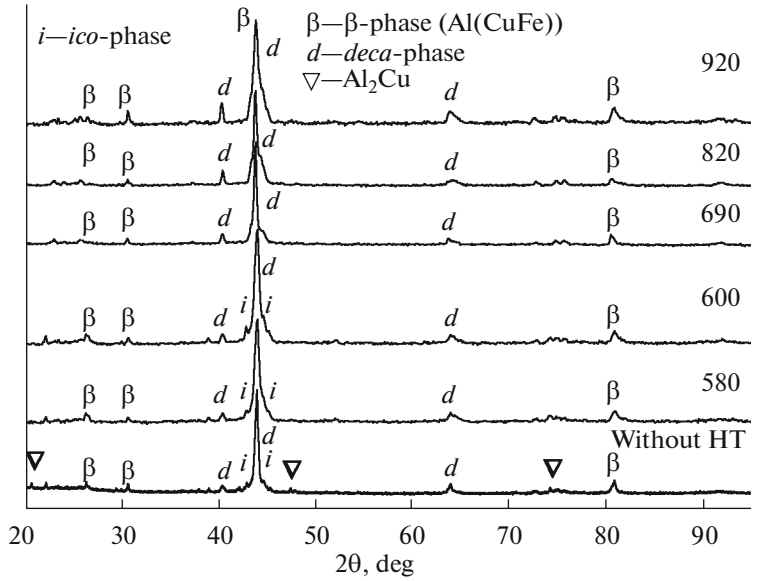

Fig. 5. X-ray powder diffraction patterns of a cast sample of the composition $Al_{65}Cu_{25}Fe_5Cr_5$ without and after heat treatments (HT) in a calorimeter (the numbers at the curves are the temperatures in °C).

Figure 6 presents the X-ray powder diffraction patterns of cast alloy $Al_{70}Cu_{20}Fe_5Cr_5$ with the highest content of QC phases after successive heatings and short-term annealings in a calorimeter to temperatures of thermal events. As is seen, with increasing annealing temperature to 740°C, the intensities of the reflections of the phase Al_2Cu decreases. At an annealing temperature of 650°C, the X-ray powder diffraction pattern shows the lines of the phase β-Al(CuFe), the intensities of which somewhat decrease with increasing heat treatment temperature. Note that, within the temperature range 550–650°C, the alloy contains ~90% *d*-phase. With increasing temperature to 900°C, the *i*-phase begins to form, and the percentage of the *d*-phase decreases to 70%.

The results of the performed studies supplemented the information on the processes ensuring the formation of QC structures in chromium-alloyed alloys in the Al–Cu–Fe ternary system after crystallization of melts and subsequent heat treatments. According to the proposed structural model of random growth, crystallization of QC phases from melt occurs by combining atomic groupings of various types [22, 23]. It was confirmed that stable quasi-crystals form in ter-

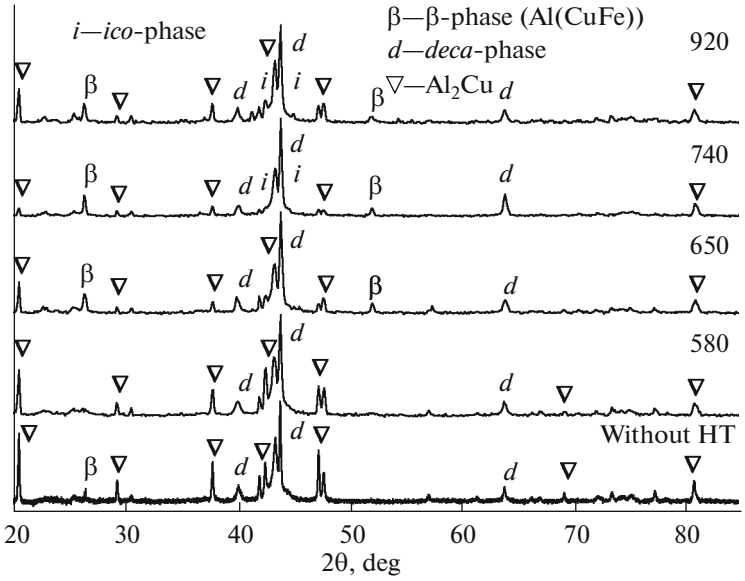

Fig. 6. X-ray powder diffraction patterns of a cast sample of the composition $Al_{70}Cu_{20}Fe_5Cr_5$ without and after heat treatments (HT) in a calorimeter (the numbers at the curves are the temperatures in °C).

nary alloys by combining atomic clusters with local ordering of the icosahedral type, which form while cooling melts. The chemical composition of a cluster with the *i*-symmetry is Al_6Cu_2Fe, which virtually coincides with the composition of phase regions in the Al–Cu–Fe ternary system [5, 8]. The chemical composition of quasi-crystals in the quaternary system is likely to be Al_7Cu_2FeCr for the *d*-phases and Al_6Cu_2FeCr for the *i*-phases, which was confirmed by the obtained experimental results of energy-dispersive X-ray spectroscopy and also the published data [17–19]. Alloying of the OC *i*-phase with chromium leads to a change in its morphology from dendritic to fine-granular multifaceted microstructure (Fig. 2). An increase in heat treatment temperature is accompanied by the polymorphic transformation $i \Leftrightarrow d$, which leads to a change not only in the morphology of grains of phases, but also to the formation of a certain QC state of the powder material.

Using a set of physicochemical analysis methods (X-ray powder diffraction analysis, scanning electron microscopy, differential scanning calorimetry), the qualitative and quantitative compositions of phases in cast alloys in the Al–Cu–Fe–Cr quaternary system were determined. The effect of temperature on the phase transitions $i \Leftrightarrow d$ in alloys $Al_{65}Cu_{25}Fe_5Cr_5$ and $Al_{70}Cu_{20}Fe_5Cr_5$ was studied,

The existence of multiphase structures being a mixture of quasi-crystalline and approximant phases, the contents and morphologies of which depend both on the composition of the initial mixture and on the crystallization rate. In the Al–Cu–Fe ternary system, after crystallization, the λ-, β-, and *i*-phases form. In alloys alloyed with 5% Cr in the Al–Cu–Fe–Cr system, the λ-phase was not found. In the sample of the composition $Al_{70}Cu_{20}Fe_5Cr_5$ with the highest content of the *d*-phase (90%), the β- and θ-phases occur as approximants.

A two-stage method was proposed for synthesizing quasi-crystalline powder materials with the decagonal structure from cast alloys in the Al–Cu–Fe–Cr quaternary system by short-term heat treatment at 600°C for 30 min.

REFERENCES

1. J. M. Dubois, Mater. Sci. Eng. **294–296**, 4 (2000).
2. M. Feuerbacher, C. Metzmacher, M. Wollgarten, et al., Mater. Sci. Eng. **233A**, 103 (1997).
3. L. I. Adeeva and A. L. Borisova, Fiz. Khim. Tv. Tela **3**, 454 (2002).
4. S. S. Kang, J. M. Dubois, and J. von Stebut, J. Mater. Res. **8**, 2471 (1993).
5. L. Zhang, J. Schneider, and R. Luck, Intermetallics **13**, 1195 (2005).
6. W. Steurer, Acta Crystallogr. **61A**, 28 (2005).
7. V. S. Kraposhin, A. L. Talis, H. T. Lam, and J. M. Dubois, J. Phys.: Condens. Matter **20**, 1 (2008).
8. L. Zhang and R. Lück, J. Alloys Compd. **342**, 53 (2002).
9. L. Zhang and R. Lück, Z. Metallkd. **94**, 774 (2003).
10. K. B. Kalmykov, N. L. Zvereva, S. F. Dunaev, et al., Vestn. Mosk. Univ., Ser. 2: Khim. 50 (2), 122 (2009).
11. D. B. Chugunov, A. K. Osipov, K. B. Kalmykov, and L. L. Meshkov, Vestn. Mosk. Univ., Ser. 2: Khim. **56** (2), 80 (2015).
12. H. Selke, U. Vogg, and P. L. Ryder, Philos. Mag., Part B **65**, 421 (1992).

13. J. Furihata and T. Okabe, J. Electron Microsc. **48**, 761 (1999).
14. Y. Qi, Z. Zhang, Z. Hei, and C. Dong, J. Alloys Compd. **285**, 221 (1999).
15. B. Grushko and T. Velikanova, Calphad **31**, 217 (2007).
16. A. P. Shevchukov, T. A. Sviridova, S. D. Kaloshkin, et al., J. Alloys Compd. **586** (Suppl. 1), S391 (2014).
17. G. Rosas and R. Perez, J. Mater. Sci. **32**, 2403 (1997).
18. W. G. Yang, R. Wang, and J. Gui, Philos. Mag. Lett. **74**, 357 (1996).
19. H. Kim, B. H. Kim, S. M. Lee, et al., J. Alloys Compd. **342**, 246 (2002).
20. T. R. Anantharaman, Bull. Mater. Sci. **21**, 71 (1998).
21. E. Huttunen-Saarivirta, J. Alloys Compd. **363**, 150 (2004).
22. A. I. Zaitsev, N. E. Zaitseva, R. Yu. Shimko, et al., J. Phys.: Condens. Matter **20**, 114 (2008).
23. C. Dong, J. B. Qiang, Y. M. Wang, et al., Philos. Mag. **86**, 263 (2006).
24. E. V. Shelekhov and T. A. Sviridova, Metalloved. Term. Obrab. Met., No. 8, 16 (2000).

Translated by V. Glyanchenko